ADJOINT MODEL CONSTRAINTS ON NH_3 SOURCES FROM REMOTE AND IN SITU OBSERVATIONS

Daven K. Henze*
Department of Mechanical Engineering, University of Colorado, Boulder, CO, USA

Mark W. Shephard, Karen E. Cady-Pereira, Vivienne Payne
AER Inc, Lexington, MA, USA

Ming Luo, Reinhard Beer
Jet Propulsion Laboratory, Pasadena, CA, USA

Robert W. Pinder, John T. Walker,
U.S. EPA, Research Triangle Park, NC, USA

1 INTRODUCTION

The detection of boundary layer ammonia by the NASA TES instrument provides unprecedented opportunity for reducing persistent uncertainties in our understanding of the distribution and impacts of atmospheric ammonia. Ammonia (NH_3) affects air quality and climate through its role in the mass, composition and physical properties of tropospheric aerosol. In order to maximize the potential of TES observations to constrain model estimates of these important processes, we will take advantage of recently developed data assimilation tools for combining remote sensing constraints with in situ measurements. The goal is to improve both spatial distributions and seasonal estimates of sources and fates of NH_x in air quality models, quantifying how this alters particle compositions and sensitivities to changing emissions.

Considerable effort will be made to first characterize the approach using model generated ("pseudo") observations, exploring the influence of prior assumptions and covariances. The inverse modeling results will be evaluated through comparison of subsequent model estimated NH_3 and $PM_{2.5}$ concentrations and with additional observations.

2 INVERSE & ADJOINTS

Sensitivity analysis of air quality models is an important aspect of analyzing model estimates and reconciling differences with observed quantities. A chemical transport model can be viewed as a sequence of discrete operators, F^n, that advances a concentration vector from time step n to step n+1,

$$\mathbf{c}^{n+1} = F^n(\mathbf{c}^n, \boldsymbol{\sigma}), \tag{1}$$

where $\mathbf{c}^n$ is the vector of all K tracer concentrations, $\mathbf{c}^n$=$[c_1^n, \ldots, c_k^n, \ldots, c_K^n]^T$ at time step n=0,...,N, and $\boldsymbol{\sigma}$ is a vector of M parameters, $\boldsymbol{\sigma} = [\sigma_1, \ldots, \sigma_m, \ldots, \sigma_M]^T$. The Jacobian matrices of the model operator around any given time step can be written as

$$\frac{\partial \mathbf{c}^{n+1}}{\partial \mathbf{c}^n} = \frac{\partial F^n(\mathbf{c}^n)}{\partial \mathbf{c}^n} \equiv \mathbf{F}_c^n, \;\; \frac{\partial \mathbf{c}^{n+1}}{\partial \boldsymbol{\sigma}} = \frac{\partial F^n(\mathbf{c}^n)}{\partial \boldsymbol{\sigma}} \equiv \mathbf{F}_\sigma^n. \tag{2}$$

An adjoint model is used to calculate the sensitivity of a single scalar model response function, $\mathcal{J}$, with respect to all model parameters, $\boldsymbol{\sigma}$. The response function includes one set of terms, $J^n(\mathbf{c}^n)$, that may depend upon only concentrations of particular species or in particular locations, and may include a second term that explicitly depends upon the parameters, $J_\sigma(\boldsymbol{\sigma})$. As specification of the exact form of these terms is not necessary for derivation of the adjoint model, the response is written in general form,

$$\mathcal{J} = \sum_{n=0}^{N} J^n(\mathbf{c}^n) + J_\sigma(\boldsymbol{\sigma}). \tag{3}$$

The adjoint sensitivity variables are defined as $\boldsymbol{\lambda}_c^n = \nabla_{\mathbf{c^n}} \mathcal{J}$ and $\boldsymbol{\lambda}_\sigma = \nabla_{\boldsymbol{\sigma}} \mathcal{J}$, where the subscripts c and σ indicate sensitivity with respect to $\mathbf{c}$ and $\boldsymbol{\sigma}$, respectively. Initializing

$$\boldsymbol{\lambda}_c^N = \frac{\partial J^N}{\partial \mathbf{c}^N} \text{ and } \boldsymbol{\lambda}_\sigma = \frac{\partial J_\sigma}{\partial \boldsymbol{\sigma}},$$

adjoint sensitivities are found by evaluating the following update formulas iteratively from n=$N, \ldots, 1$,

$$\boldsymbol{\lambda}_c^{n-1} = (\mathbf{F}_c^{n-1})^T \boldsymbol{\lambda}_c^n + \frac{\partial J^{n-1}}{\partial \mathbf{c}^{n-1}}, \tag{4}$$

$$\boldsymbol{\lambda}_\sigma = (\mathbf{F}_\sigma^{n-1})^T \boldsymbol{\lambda}_c^n + \boldsymbol{\lambda}_\sigma, \tag{5}$$

at the conclusion of which $\boldsymbol{\lambda}_c^0$ is the sensitivity of the cost function with respect to initial conditions, $\nabla_{\mathbf{c^0}} \mathcal{J}$, and $\boldsymbol{\lambda}_\sigma$ is the desired sensitivity of the cost function with respect to the model parameters, $\nabla_{\boldsymbol{\sigma}} \mathcal{J}$. The adjoint model calculates the sensitivity of the scalar model response with respect to all M

*daven.henze@colorado.edu

elements of the model parameter vector in ∼3 times the length of a forward model run, which is nearly M times more efficient than finite difference or decoupled direct methods. Given M can be $\mathcal{O}(10^5)$ for a 3-D air quality model, the savings are considerable.

Data assimilation techniques provide a framework for combining observations and models to form an optimal estimate of the state of a system, which in this case is the chemical makeup of the troposphere. To start with, a range of models is typically constructed using control variables, $\boldsymbol{\sigma}$, to adjust elements of the vector of model parameters, $\mathbf{p}$, via application as scaling factors, $p = p_a e^{\sigma}$, where $\mathbf{p_a}$ is the prior parameter estimate. The approach we consider iteratively employs the adjoint of an air quality model in a method referred to as 4D-Var (Sandu et al., 2005), used here for inverse modeling of emissions. The advantage of this method is that numerous ($\mathcal{O}(10^5)$) model parameters can be optimized simultaneously while still retaining the constraints of the full forward model physics and chemistry. This approach to inverse modeling seeks $\boldsymbol{\sigma}$ that minimizes the cost function, $\mathcal{J}$, given by

$$\begin{aligned} \mathcal{J} &= \frac{1}{2}\sum_{\mathbf{c}\in\Omega}(H\mathbf{c}-\mathbf{c}_{obs})^T\mathbf{S}_{obs}^{-1}(H\mathbf{c}-\mathbf{c}_{obs}) \\ &+ \frac{1}{2}(\boldsymbol{\sigma}-\boldsymbol{\sigma}_a)^T\mathbf{S}_a^{-1}(\boldsymbol{\sigma}-\boldsymbol{\sigma}_a) \end{aligned} \quad (6)$$

where H is the observation operator, $\boldsymbol{\sigma}_a$ is the prior estimate of the control variables, $\mathbf{S}_a$ and $\mathbf{S}_{obs}$ are error covariance estimates of the control variables and observations, respectively, and Ω is the domain over which observations, $\mathbf{c}_{\text{obs}}$, and model predictions are available. Overall, the cost function is a specific model response, the minimum value of which balances the objectives of improving model performance while ensuring the model itself remains within a reasonable range (as dictated by $\mathbf{S}_a^{-1}$) of the initial model. Gradients of the cost function with respect to the parameter scaling factors calculated with the adjoint model, $\nabla_{\boldsymbol{\sigma}}\mathcal{J}$, are supplied to an optimization routine (the quasi-Newton L-BFGS-B optimization routine (Byrd et al., 1995; Zhu et al., 1994)), and the minimum of the cost function is sought iteratively. At each iteration, improved estimates of the model parameters are implemented and the forward model solution is recalculated.

3 MODELING

GEOS-Chem GEOS-Chem is a chemical transport model driven using assimilated meteorology from the Goddard Earth Observing System (GEOS) of the NASA Global Modeling and Assimilation Office (Bey et al., 2001). GEOS-Chem includes an online secondary inorganic aerosol simulation introduced and described in full by Park et al. (2004). Model estimates of inorganic $PM_{2.5}$ have been compared to surface measurements (Park et al., 2004, 2006; Liao et al., 2007; Henze et al., 2009; Pye et al., 2009) and measurements from aircraft campaigns (Heald et al., 2005, 2006); NH_3 emissions are frequently indicated to be a likely cause of discrepancies.

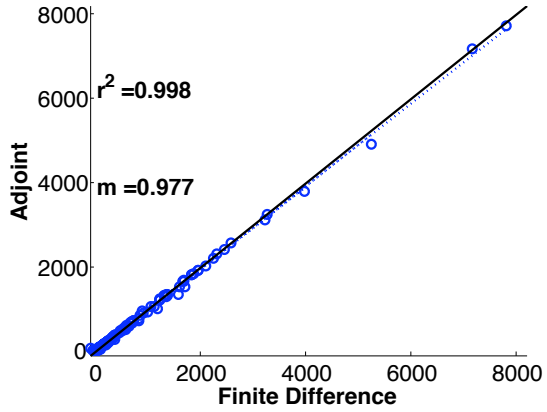

(a)

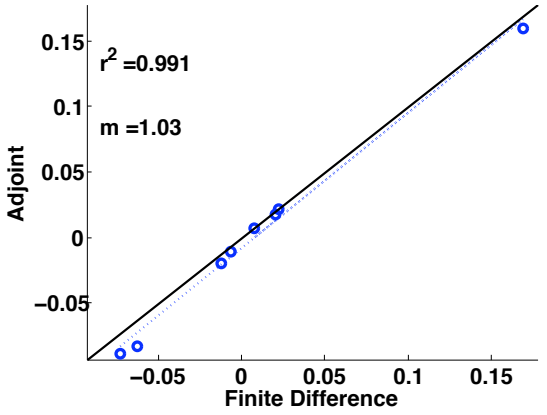

(b)

Figure 1: Validation of adjoint model sensitivities via comparison to finite difference (FD) results for week-long simulations. Solid lines are 1:1, dashed are regressions with given r^2 and slope m. (a) Global tests of the 1-D adjoint model: sensitivities of nitrate aerosol with respect to NH_3 emissions. (b) Spot tests of the full adjoint model: change in direct aerosol radiative forcing from perturbations (positive and negative) to SO_2 emissions in eight different locations.

GEOS-Chem adjoint model The adjoint of the GEOS-Chem model was developed specifically for inverse modeling of precursors of inorganic $PM_{2.5}$ with explicit inclusion of gas-phase chemistry, heterogeneous chemistry, and treatment of the ther-

modynamic couplings of the sulfate - ammonium - nitrate - water aerosol system (Henze et al., 2007, 2009). As the only adjoint model to explicitly represent this system, it is uniquely capable of exploiting speciated measurement of both gaseous and particulate components in novel ways. The accuracy of the adjoint model calculations are verified through extensive comparisons of adjoint to finite difference sensitivities, as shown in Fig. 1. In order to maximize points of comparison between these two approaches, we consider both ensembles of 1-D models (i.e., no horizontal transport) as well as spot tests of the full 3-D adjoint model (testing the full adjoint model for each parameter is not feasible, as it would require $M + 1$ forward model calculations).

4 OBSERVATIONS

Remotely sensed NH_3 observations from TES The high spectral resolution and good signal-to-noise ratio of the TES instrument (Shephard et al., 2008) have enabled the first detection of tropospheric ammonia from space, recently demonstrated over Southern California and China (Beer et al., 2008). TES is an infrared Fourier transform spectrometer with spectral resolution of 0.06 cm^{-1} aboard the NASA Aura satellite, launched July 15, 2004 (Schoeberl et al., 2006). TES global survey observations repeat with a 16-day cycle and have a nadir footprint of 5 km $\times$ 8 km; for example, that is about $\sim$2000 scenes a month over North America after cloud screening (optical depths < 1.0) and applying the TES retrieval quality control flags. NH_3 retrievals are scheduled to become implemented in the TES operational retrieval algorithm as a standard product in 2010. At this time the TES retrievals will be both processed forward in time and reprocessed from the implementation period back to the start of the TES observations in July 2004. The TES science team also schedules and accepts proposals for additional high density measurements (Special Observations), such as the Transect mode with 40 continuous observations of 12 km footprints covering $\sim$480 km.

The TES retrievals use an optimal estimation method, which has the advantage of directly providing the averaging kernel, $\mathbf{A}$, and inverse error covariance matrix, $\mathbf{S}_{obs}^{-1}$, needed for subsequent inverse modeling. The averaging kernel describes the sensitivity of the retrieval to the true atmospheric state. The sum of each row of $\mathbf{A}$ can be used as a metric to estimate the fraction of information in the retrieval that comes from the measurement rather than the

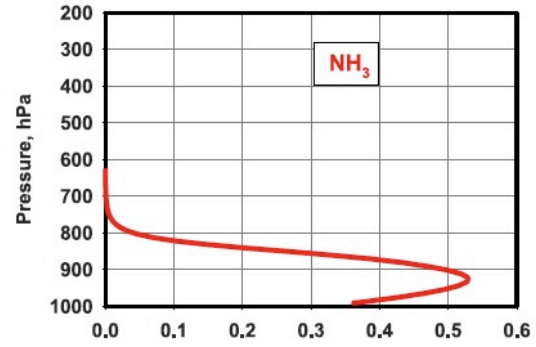

(a)

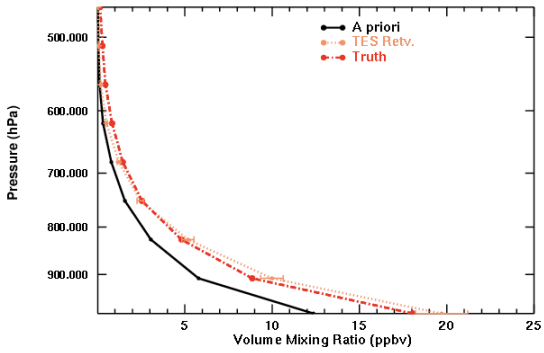

(b)

Figure 2: (a) TES instrumental sensitivity (sum of the rows of the averaging kernel) to NH_3, demonstrating boundary layer detection capabilities (figure from Beer et al., 2008). (b) Recovery of a "true" profile of NH_3 by the TES retrieval when starting from a prior NH_3 profile generated from a simulation with NH_3 emissions half the magnitude of those used to generate the Truth.

a priori (Rodgers, 2000) at the corresponding altitude. An example of the sum of the rows for the TES NH_3 retrieval over Beijing China (Beer et al., 2008) is provided in Fig. 2(a). The vertical resolution is defined as the full-width-half-maximum of the row of the averaging kernel. In this example the vertical resolution is approximately 2 km from near surface to $\sim$800 mb ($\sim$2 km) with peak sensitivity at $\sim$900 mb ($\sim$1km). Note that the sensitivity of the TES retrieval does vary from profile-to-profile as it may be affected by the signal-to-noise ratio (and therefore by the concentration of NH_3), by clouds, and by the retrieval constraints.

Comparison of model estimates to satellite observations is done via application of the following formula for the TES observational operator, H,

$$H\mathbf{c} = \mathbf{c}_a + \mathbf{A}(\mathbf{M}\mathbf{c} - \mathbf{c}_a) \qquad (7)$$

where $\mathbf{c}$ is the model estimated NH_3 profile, $\mathbf{M}$ is a matrix that maps these values to the retrieval units and vertical levels, $\mathbf{c}_a$ is the a priori NH_3 profile used

for the retrieval. By comparing TES NH_3 profiles to mapped model estimates, $H\mathbf{c}$, rather than the native model NH_3 profile, $\mathbf{c}$, the contribution of error in $\mathbf{c}_a$ to the measurement error, $\mathbf{S}_{obs}$, cancels out (Rodgers, 2000).

As a test of the contribution of a priori model estimates of the atmospheric distribution and variability of NH_3 to the satellite retrievals, perturbed NH_3 model fields are also generated that differ from the standard fields used as prior constraints for the NH_3 retrieval. TES NH_3 observations are then simulated based on radiative transfer calculations from the perturbed fields and the retrieval algorithm is applied, beginning with unperturbed profiles, verifying that the "true" profile can be recovered. An example of this process is given in Fig. 2(b).

Surface measurements We will make use of speciated measurements from monitoring stations such as STN (*http://www.epa.gov/ttnamti1/specgen.html*), CASTNet (Baumgardner et al., 2002), and IMPROVE (Malm et al., 2004) to provide observations of sulfate, nitrate, and ammonium at several hundred locations within the U.S. These measurements are collected on a one in three or one in six cycle for STN and IMPROVE sites, and on a weekly basis for CASTNet sites. Following guidelines for using speciated $PM_{2.5}$ networks measurements (EPA, 2007; Frank, 2006), we will avoid known issues with NH_4^+ from STN and NO_3^- from CASTNet by using measurements of NH_4^+ from CASTNet, NO_3^- from STN, and SO_4^{2-} and NO_3^- from IMPROVE. Wet deposited NH_x will be taken from the National Atmospheric Deposition Program National Trends Network (NADP/NTN) collected weekly at ∼200 stations throughout the U.S. Following Gilliland et al. (2006), a 10% upward correction will be applied to account for sample degradation.

5 CONSTRAINING US NH_3 SOURCES

The first step of this phase of the project will be to explore the capabilities and limitations of the global inverse modeling setup in idealized control conditions by designing inverse problems with known solutions. An example is presented for an inverse modeling test where pseudo-observations of NH_3 from TES and sulfate and nitrate from IMPROVE were generated using a model with doubled NH_3 emissions. For these tests, 87 pseudo TES observations were used from July 14-19, 2005, along roughly a dozen global survey transects crossing the midwestern U.S. NH_3 emissions scaling factors ($\sigma = ln(E/E_0)$) after only four iterations of the inverse model are shown in Fig. 3(a). These scaling factors were zero at the first iteration, but were 0.69 ($=ln(2)$) when generating the pseudo-observations. While clearly further optimization is warranted, this simple example shows that the inverse model is quickly converging to a simulation that reproduces the observations (cost function decreased by 83%) by adjusting the scaling factors towards the truth. Incorrect compensation through adjustment of scaling factors for emissions of SO_2 and NO_x was minimal. Further, results were markedly improved compared to another test using only the IMPROVE observations (cost function decreased by 61%), with more uniform progression of the scaling factors toward the correct value when using TES observations. For the actual proposed research, we will consider a wide range of perturbations (not just a domain wide factor of two), longer time periods, more pseudo-observations and higher resolution simulations, exploring the dependence of convergence to the correct solution on the amount and quality of the observation and prior information provided to the inverse model. The impact on the inversion's accuracy of a priori values and covariance constraints in the TES retrieval itself will be explored through repeated tests altering these parameters.

A demonstration of how much information regarding NH_3 emissions can be extracted from a single track of TES NH_3 observations is given in Fig. 3(b). Here we calculate the sensitivity of a single set of model estimated NH_3 retrievals, $H\mathbf{c}$, to anthropogenic NH_3 emissions over the course of several previous days with the GEOS-Chem adjoint running at $2^\circ \times 2.5^\circ$. The results are normalized to the maximum sensitivity, in yellow, and the location of the TES footprints along the track are marked with green $\mathbf{x}$'s. Owing to the dependence of the modeled NH_3 in those places on the amount of NH_x, and hence the amount of aerosol ammonium sulfate and ammonium nitrate having in part come from distant emissions, the influence is seen to be quite widespread.

For an application with real data, we will use TES observations throughout 2009 and compare these to model estimates from the GEOS-Chem chemical transport model in a global $2^\circ \times 2.5^\circ$ simulation. To estimate error covariances of the prior NH_3 emissions we will draw from literature describing the variability and uncertainty in NH_3 emissions. For example, the work of Beusen et al. (2008) defines groups of land-types relevant to NH_3 emissions that can be used to construct spatial correlation length scales

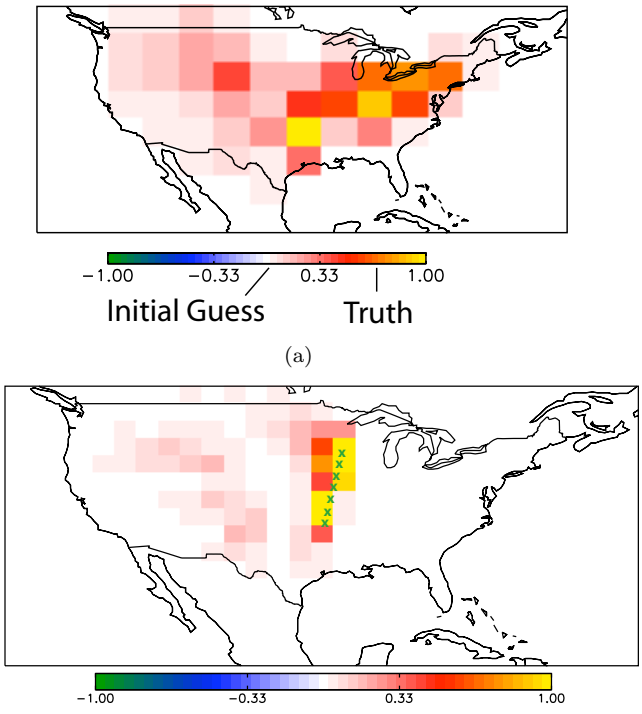

Figure 3: (a) Progress towards optimizing the NH_3 emissions after four iterations using all pseudo-observations. (b) Sensitivity of model estimated NH_3 profiles ($H\mathbf{c}$) along a single track of actual TES footprints (marked with $\mathbf{x}$'s) with respect to NH_3 emissions from the prior week. Sensitivities are scaled relative to maximum values (yellow).

for NH_3 emissions. Studies such as Stephen and Aneja (2008) also give guidance on the likely spatial variability of NH_3 emissions. Inversion of the error covariance matrix will be calculated using matrix factorization algorithms as in the 4D-var study of Chai et al. (2007). The minimization of the cost function will be considered to have converged when the magnitude of the gradient norm has decreased by more than an order of magnitude and/or the cost function has ceased to change significantly at subsequent iterations.

We will also use additional air quality network measurements of sulfate and nitrate, where available (Sec. 4), to both constrain the inversion and provide a means of evaluating the inverse modeling solutions through cross validation, wherein some of the observational data is withheld during the inversion to be used afterwards an independent check on the optimized solution. Uncertainty and error correlations of the solution will be estimated from the approximate inverse Hessian gleaned from the minimization procedure (e.g., Muller and Stavrakou, 2005; Henze et al., 2009). This approach to quantifying posterior uncertainty utilizes the fact that well constrained values correspond to sharp minimums in the cost function while less constrained values have shallow minimums. Possible biases owing to the initial guess will be identified by restarting the inversion using a different set of NH_3 emissions and noting if this alters the solution.

References

Baumgardner, R. E., T. F. Lavery, C. M. Rogers, and S. S. Isil, 2002: Estimates of the atmospheric deposition of sulfur and nitrogen species: Clean air status and trends network, 1990-2000. *Environ. Sci. Technol.*, **36**, 2614–2629.

Beer, R., M. W. Shephard, S. Kulawik, S. A. Clough, R. A. Eldred, K. W. Bowman, S. P. Sander, B. M. Fisher, V. H. Payne, M. Louo, G. B. Osterman, and J. R. Worden, 2008: First satellite observations of lower tropospheric ammonia and methanol. *Geophys. Res. Lett.*, **35**, doi:10.1029/2008GL033642.

Beusen, A. H. W., A. F. Bouwman, P. S. C. Heuberger, G. Van Drecht, and K. W. Van Der Hoek, 2008: Bottom-up uncertainty estimates of global ammonia emissions from global agricultural production systems. *Atmos. Environ.*, **42**, 6067–6077.

Bey, I., D. J. Jacob, R. M. Yantosca, J. A. Logan, B. D. Field, A. M. Fiore, Q. B. Li, H. G. Y. Liu, L. J. Mickley, and M. G. Schultz, 2001: Global modeling of tropospheric chemistry with assimilated meteorology: Model description and evaluation. *J. Geophys. Res.-Atmos.*, **106**, 23073–23095.

Byrd, R. H., P. H. Lu, J. Nocedal, and C. Y. Zhu, 1995: A limited memory algorithm for bound constrained optimization. *Siam J. Sci. Comput.*, **16**, 1190–1208.

Chai, T. F., G. R. Carmichael, Y. H. Tang, A. Sandu, M. Hardesty, P. Pilewskie, S. Whitlow, E. V. Browell, M. A. Avery, P. Nedelec, J. T. Merrill, A. M. Thompson, and E. Williams, 2007: Four-dimensional data assimilation experiments with International Consortium for Atmospheric Research on Transport and Transformation ozone measurements. *J. Geophys. Res.-Atmos.*, **112**, –, doi:10.1029/2006jd007763.

EPA, 2007: Guidance on the use of models and other analyses for demonstrating attainment of air qual-

ity goals for ozone, $PM_{2.5}$, and regional haze. *EPA -454/B-07-002*.

Frank, N. H., 2006: Retained nitrate, hydrated sulfates, and carbonaceous mass in federal reference method fine particulate matter for six eastern us cities. *J. Air Waste Manage. Assoc.*, **56**, 500–511.

Gilliland, A. B., K. W. Appel, R. W. Pinder, and R. L. Dennis, 2006: Seasonal NH_3 emissions for the continental United States: Inverse model estimation and evaluation. *Atmos. Environ.*, **40**, 4986–4998.

Heald, C. L., D. J. Jacob, R. J. Park, L. M. Russell, B. J. Huebert, J. H. Seinfeld, H. Liao, and R. J. Weber, 2005: A large organic aerosol source in the free troposphere missing from current models. *Geophys. Res. Lett.*, **32**, doi:10.1029/2005GL023831.

Heald, C. L., D. J. Jacob, S. Turquety, R. C. Hudman, R. J. Weber, A. P. Sullivan, R. E. Peltier, E. L. Atlas, J. A. de Gouw, C. Warneke, J. S. Holloway, J. A. Neuman, F. M. Flocke, and J. H. Seinfeld, 2006: Concentrations and sources of organic carbon aerosols in the free troposphere over North America. *J. Geophys. Res.-Atmos.*, **111**, doi:10.1029/2006JD007705.

Henze, D. K., A. Hakami, and J. H. Seinfeld, 2007: Development of the adjoint of GEOS-Chem. *Atmos. Chem. Phys.*, **7**, 2413–2433.

Henze, D. K., J. H. Seinfeld, and D. Shindell, 2009: Inverse modeling and mapping U.S. air quality influences of inorganic $PM_{2.5}$ precursor emissions using the adjoint of geos-chem. *Atmos. Chem. Phys.*, **9**, 5877–5903.

Liao, H., D. K. Henze, J. H. Seinfeld, S. Wu, and L. J. Mickley, 2007: Biogenic secondary organic aerosol over the United States: Comparison of climatological simulations with observations. *J. Geophys. Res.-Atmos.*, **112**, doi:10.1029/2006JD007813.

Malm, W. C., B. A. Schichtel, M. L. Pitchford, L. L. Ashbaugh, and R. A. Eldred, 2004: Spatial and monthly trends in speciated fine particle concentration in the United States. *J. Geophys. Res.-Atmos.*, **109**, doi:10.1029/2003jd003739.

Muller, J. F. and T. Stavrakou, 2005: Inversion of CO and NO_x emissions using the adjoint of the IMAGES model. *Atmos. Chem. Phys.*, **5**, 1157–1186.

Park, R. J., D. Jacob, B. D. Field, R. Yantosca, and M. Chin, 2004: Natural and transboundary pollution influences on sulfate-nitrate-ammonium aerosols in the United States: Implications for policy. *J. Geophys. Res.-Atmos.*, **109**, doi:10.1029/2003JD004473.

Park, R. J., D. J. Jacob, N. Kumar, and R. M. Yantosca, 2006: Regional visibility statistics in the United States: Natural and transboundary pollution influences, and implications for the Regional Haze Rule. *Atmos. Environ.*, **40**, 5405–5423.

Pye, H. O. T., H. Liao, S. Wu, L. J. Mickley, D. J. Jacob, D. K. Henze, and J. H. Seinfeld, 2009: Effets of changes in climate and emissions on future sulfate-nitrate-ammonium aerosol levels in the United States. *J. Geophys. Res.-Atmos.*, **114**, doi:10.1029/2008JD010701.

Rodgers, C. D., 2000: *Inverse Methods for Atmospheric Sounding*, volume 2 of *Series on Atmospheric, Oceanic and Planetary Physics*. World Scientific, Singapore.

Sandu, A., D. N. Daescu, G. R. Carmichael, and T. F. Chai, 2005: Adjoint sensitivity analysis of regional air quality models. *J. Comput. Phys.*, **204**, 222–252.

Schoeberl, M. R., A. R. Douglass, E. Hilsenrath, P. K. Bhartia, R. Beer, J. W. Waters, M. R. Gunson, L. Froidevaux, J. C. Gille, J. J. Barnett, P. E. Levelt, and P. DeCola, 2006: Overview of the EOS Aura mission. *Ieee Transactions on Geoscience and Remote Sensing*, **44**, 1066–1074, doi:10.1109/Tgrs.2005.861950.

Shephard, M. W., H. M. Worden, K. E. Cady-Pereira, M. Lampel, M. Z. Luo, K. W. Bowman, E. Sarkissian, R. Beer, D. M. Rider, D. C. Tobin, H. E. Revercomb, B. M. Fisher, D. Tremblay, S. A. Clough, G. B. Osterman, and M. Gunson, 2008: Tropospheric emission spectrometer nadir spectral radiance comparisons. *J. Geophys. Res.-Atmos.*, **113**, doi:10.1029/2007jd008856.

Stephen, K. and V. P. Aneja, 2008: Trends in agricultural ammonia emissions and ammonium concentrations in precipitation over the Southeast and Midwest United States. *Atmos. Environ.*, **42**, 3238–3252.

Zhu, C., R. H. Byrd, P. Lu, and J. Nocedal, 1994: L-BFGS-B: A limited memory FORTRAN code for solving bound constrained optimization problems. Technical report, Northwestern University.